

Order-disorder $c(4 \times 2)$ - (2×1) transition on Ge(001): An *in situ* x-ray scattering study

C. A. Lucas

*Materials Science Division, Center for Advanced Materials, Lawrence Berkeley Laboratory,
University of California, Berkeley, California 94720*

C. S. Dower

Department of Physics, University of Edinburgh, Edinburgh EH9 3JZ, United Kingdom

D. F. McMorrow

Department of Physics, Clarendon Laboratory, University of Oxford, Oxford OX1 3PU, United Kingdom

G. C. L. Wong

*Materials Science Division, Center for Advanced Materials, Lawrence Berkeley Laboratory,
University of California, Berkeley, California 94720
and Department of Physics, University of California, Berkeley, California 94720*

F. J. Lamelas and P. H. Fuoss

AT&T Bell Laboratories, 600 Mountain Avenue, Murray Hill, New Jersey 07974

(Received 3 December 1992)

Using *in situ* x-ray diffraction, we have studied the order-disorder phase transition on the Ge(001) surface by measuring the temperature dependence of a superlattice reflection specific to the $c(4 \times 2)$ low-temperature phase. The results indicate that the transition corresponds to a two-dimensional phase transition with anisotropic interaction energies along and perpendicular to the dimer rows that form the (2×1) surface. Due to pinning of the $c(4 \times 2)$ domains by defects, we are unable to observe any universal critical behavior. The results indicate that the number of buckled dimers involved in the $c(4 \times 2)$ reconstruction is conserved through the transition. This implies that above room temperature the (2×1) surface consists of a random array of buckled dimers.

I. INTRODUCTION

The Ge(001) surface is similar to the Si(001) surface and exhibits a two-domain (2×1) reconstruction, which consists of rows of atomic dimers created through the pairing of nearest-neighbor surface atoms.¹ Recently there has been considerable controversy over the exact nature of the dimer, i.e., whether it is symmetric or asymmetric,² and therefore over the amount of charge transfer across the dimer.³⁻⁵ The asymmetric dimer has an axis that is inclined to the surface plane: one atom buckles away from the surface and one buckles in. This asymmetry allows for higher-order reconstructions, such as $p(2 \times 2)$, $c(2 \times 2)$, and $c(4 \times 2)$, which were predicted on the basis of energy-minimization calculations⁶ and have since been observed by ion scattering,⁷ scanning-tunneling microscopy (STM),^{8,9} low-energy electron diffraction (LEED),¹⁰ and helium scattering.¹¹

By considering the buckled dimer as an Ising-spin variable and using a renormalization-group calculation, Ihm *et al.*¹² predicted an order-disorder transition of the Si(001) surface below room temperature. A $c(4 \times 2) \rightarrow (2 \times 1)$ transition was observed by LEED on Si(001) and appeared to be a reversible second-order transition occurring over a fairly wide temperature range.¹³ A similar transition on Ge(001) was observed in a LEED study by Kevan and Stoffel.¹⁴ They also observed a

metal-insulator transition at the same temperature as the structural transition, using angle-resolved photoemission. The phase transition appeared to be much sharper than for Si(001) but occurred in two stages: ordering along the dimer rows followed by ordering of the rows with respect to each other. The results led to calculations of the intermediate phase using the next-nearest-neighbor Ising model^{15,16} and estimation of the order parameter β using the LEED data.¹⁷ Despite this interest there has been no successful measurement of the critical scattering associated with the phase transition. The coherence length in LEED precludes its use as the system nears the transition temperature and the correlation length diverges.

In this paper we describe *in situ* x-ray scattering measurements of the $c(4 \times 2) \rightarrow (2 \times 1)$ phase transition on Ge(001). Although the results indicate that the surface undergoes a two-dimensional (2D) phase transition we are unable to observe any universal critical behavior due to saturation of the $c(4 \times 2)$ domain size, which we attribute to the presence of defects or impurities on the surface. The transition appears to be single-stage with very different interaction energies along and perpendicular to the dimer rows. The structure factors of the $c(4 \times 2)$ phase are consistent with the presence of asymmetric dimers and the results indicate that these asymmetric dimers are conserved through the phase transition. The paper is organized as follows. In Sec. II we describe the ex-

perimental procedure and sample preparation. In Sec. III we present the low-temperature results and in Sec. IV we relate these results to the 2D Ising model. In Sec. V we explore the structural information that is contained in the results, and we present the overall conclusions in Sec. VI.

II. EXPERIMENTAL DETAILS

The experiment was performed on beamline X16A of the National Synchrotron Light Source (NSLS) at Brookhaven National Laboratory, using an ultrahigh vacuum (UHV) chamber, equipped with LEED, coupled to a five-circle diffractometer.¹⁸ The germanium wafer (surface dimensions $\sim 18 \times 18 \text{ mm}^2$) was miscut by $< 0.1^\circ$ to the (001) lattice planes (the miscut was approximately along the [110] bulk crystallographic direction) as determined by x-ray diffraction prior to the experiment. After loading into the UHV chamber the sample surface was cleaned by repeated cycles of sputtering and annealing (0.5 h with 800-eV Ar^+ ions, followed by a 5-min anneal at 700°C and cooling at $\sim 30^\circ/\text{min}$ to room temperature) until there was no reduction in the widths of the (2×1) Bragg reflections measured by x-ray diffraction. This required approximately eight cycles [the LEED showed a sharp (2×1) pattern after only two cycles]. Slower cooling of the sample after the 700°C anneal did not improve the (2×1) domain size or the intensities of the superlattice reflections. The sample was cooled below room temperature by thermal contact with a liquid-nitrogen reservoir at a rate of $1^\circ/\text{min}$ to a minimum temperature of 170 K and the temperature was controlled by resistive heating in a feedback loop with a thermocouple in contact with a Ta ring attached to the back of the sample. Although an accurate temperature reading could not be obtained the temperature could be controlled to $\pm 2^\circ$ (from nonvacuum tests of the thermocouple reading we estimate the systematic error in the temperature to be no worse than $\pm 10 \text{ K}$). The pressure in the UHV chamber during the phase-transition experiment was $3 \times 10^{-11} \text{ Torr}$.

Following a 500-K anneal, measurements were performed as the sample was cooled by reducing the heating current. Several cycles of annealing and cooling were performed. Some of the data points were checked by cooling directly to a certain temperature after the anneal: the measurements were always found to be reproducible. It was not possible to perform the experiment by cooling to the minimum temperature ($\sim 170 \text{ K}$) with the heater current off and then heating the sample, as the pressure burst caused by switching on the heater current was sufficient to suppress the $c(4 \times 2)$ reconstruction. All measurements were made with a monochromatic x-ray beam ($\lambda = 1.238 \text{ \AA}$) focused to a 1.0 mm (horizontal) $\times 1.5 \text{ mm}$ (vertical) spot on the sample. The sample was mounted with its surface normal in the horizontal plane and slits were used to define the resolution along the surface normal. Scattered x rays were detected by a position-sensitive detector after passing through a 50 mm (horizontal) $\times 1 \text{ mm}$ (vertical) entrance slit at a distance of $\sim 500 \text{ mm}$ from the sample. The detector was binned to

give an angular resolution of $\sim 0.35^\circ$ in the horizontal scattering plane (i.e., along the sample surface normal). Full details of the diffractometer design and instrumental resolution have been discussed elsewhere.¹⁸⁻²⁰ A monitor, sampling a small fraction of the incident-beam intensity, was used to normalize the results.

The (2×1) reconstructed surface gives rise to scattering at half-integer positions in a reciprocal lattice associated with a surface tetragonal unit cell that is related to the conventional cubic unit cell by the transformations $(100)_{\text{surf}} = \frac{1}{2}(2\bar{2}0)_{\text{cub}}$, $(010)_{\text{surf}} = \frac{1}{2}(220)_{\text{cub}}$, and $(001)_{\text{surf}} = (001)_{\text{cub}}$. This is the standard LEED notation for the unit cell and the l index is dropped in the subsequent analysis. Both the (2×1) and the 90° -rotated (1×2) domains (separated by monolayer steps on the surface) were observed and the integrated intensities of their respective Bragg reflections indicated that the populations of the two domains were approximately equal (the ratio was 48:52). All surface diffraction measurements were performed at $l = 0.05$ reciprocal-lattice units (rlu), corresponding to an out-of-plane momentum transfer of $\sim 0.055 \text{ \AA}^{-1}$. At this momentum transfer the incident and exit angles of the x-ray beam to the sample surface were $\sim 0.3^\circ$, slightly above the critical angle for total external reflection. Rocking scans (ϕ scans) through the (2×1) superlattice reflections had Lorentzian line shapes corresponding to an exponential correlation function describing the domain distribution on the surface. With the detector integrating over one in-plane direction, the domain sizes are calculated by²¹

$$D = a / (\pi \Delta h_{\text{HWHM}}) \text{ \AA} , \quad (1)$$

where D is the domain size, a is the Ge lattice parameter (4 \AA along the [10] and [01] directions), and Δh_{HWHM} (or Δk_{HWHM}), the half-width at half maximum (HWHM), is in reciprocal-lattice units and was measured on the (1.50) , (1.50) , (01.5) , and $(0\bar{1}.5)$ peaks as a check of consistency. Equation (1) gives values of $\sim 1000 \text{ \AA}$ for the domain sizes along both the [10] and [01] directions. This implies that the steps on the surface are primarily of monolayer height. The calculated miscut for monolayer steps and 1000-\AA domains is 0.08° , in agreement with the measured miscut.

III. RESULTS

On cooling the sample to 170 K a strong $c(4 \times 2)$ LEED pattern and its 90° -rotated symmetry equivalent $c(2 \times 4)$ were observed. Schematic illustrations of the $c(4 \times 2)$ unit cell and the corresponding reciprocal-space x-ray scattering are shown in Figs. 1(a) and 1(b), respectively. It is important to note that two $c(4 \times 2)$ unit cells can be present on the surface, related to each other by a translation vector of magnitude $2a$ along the [10] direction. The $c(4 \times 2)$ reconstruction can therefore have an antiphase domain structure within a single terrace. Alternate terraces have 90° rotations of both domains. Figures 2(a) and 2(b) show x-ray-diffraction scans through the $(1.750.5)$ surface reflection, specific to the $c(4 \times 2)$ phase, taken at $T = 170 \text{ K}$ (the minimum temperature which could be reached with the experimental setup) and

$T=265$ K (just below room temperature). At $T=170$ K typical signal rates on the $(1.75\ 0.5)$ peak were ~ 110 counts per second (cps) on a background of ~ 30 cps. This compares with ~ 5000 cps measured at the $(1.5\ 0)$ peak. The scan directions are indicated in Fig. 1(b), which shows the peak positions for a single-domain

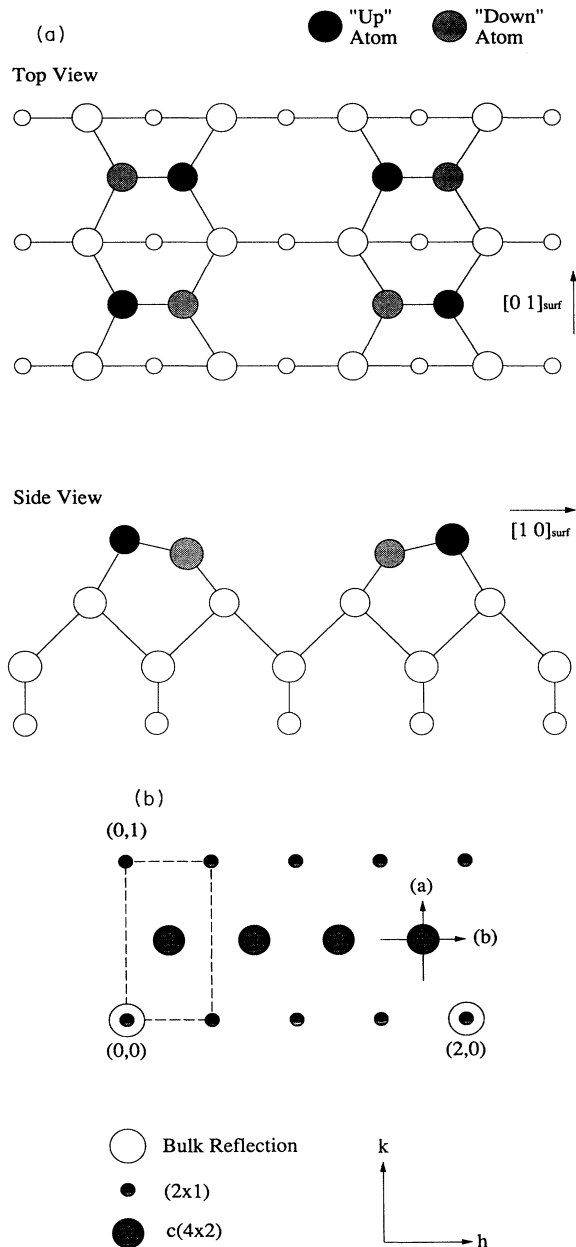


FIG. 1. (a) Schematic representation of the real-space structure for a single $c(4\times 2)$ unit cell and (b) the corresponding reciprocal-space x-ray scattering for a single-domain $c(4\times 2)$ reconstruction. Measurements of the peak at $(1.75\ 0.5)$ are described in this paper. The scan directions for the results in Figs. 2(a) and 2(b) are shown. It should be noted that there is also bulk scattering from the crystal truncation rods of out-of-plane Bragg reflections at all integer positions. The bulk scattering shown is only for in-plane allowed Bragg reflections.

$c(4\times 2)$ surface, i.e., no $c(2\times 4)$ scattering. The solid lines in Figs. 2(a) and 2(b) are fitted Lorentzian line shapes with a linear sloping background along the $[0\ 1]$ direction [Fig. 2(a)] and a constant background plus a Lorentzian centered at $h=2$ for scans along the $[1\ 0]$ direction [Fig. 2(b)]. The background was also measured at temperatures where no significant $c(4\times 2)$ peak was observed (~ 500 K) and it is assumed that the scattering is either from the bulk Ge crystal or from the tails of the half-integer (2×1) reflections which are present over the entire measured temperature range (170–500 K). Using Eq. (1) the domain sizes at $T=170$ K are 200 Å along the $[0\ 1]$ direction and 50 Å along $[1\ 0]$. These are much smaller than the (2×1) domain sizes. This implies that the $c(4\times 2)$ reconstruction still consists of antiphase domains and has not fully ordered into a single-domain $c(4\times 2)$ surface.

Figure 3 shows the measured HWHM's along the scan directions shown in Fig. 1(b) through the $(1.75\ 0.5)$ peak

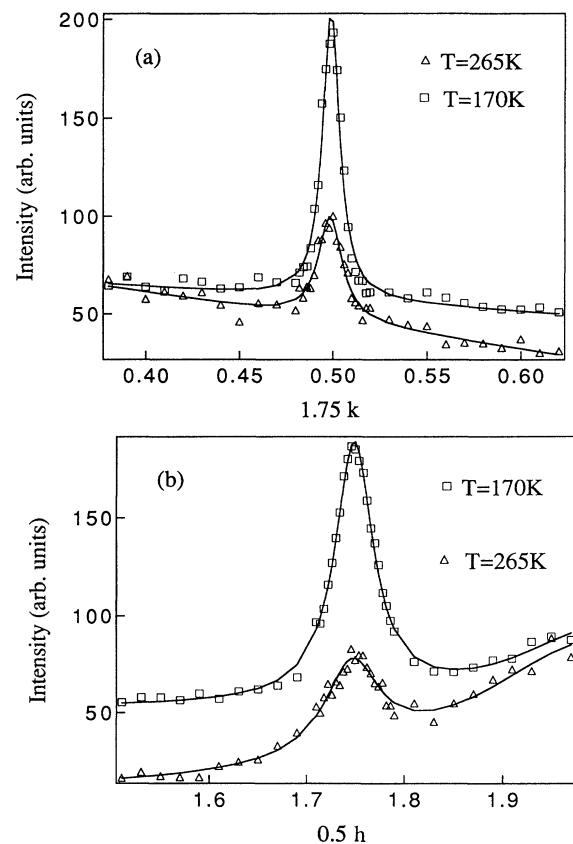


FIG. 2. Scans through the $(1.75\ 0.5)$ reflection (a) along the $[0\ 1]$ direction and (b) along the $[1\ 0]$ direction for two temperatures $T=170$ K and $T=265$ K. The data sets for the two different temperatures are displaced for clarity. At $T=170$ K the background count rate in Fig. 2(a) was typically 30 cps. It is approximately twice as high in the scans at $T=265$ K. Solid lines are Lorentzian line shapes with a linear sloping background in (a) and a constant background plus a Lorentzian centered at $h=2$ in (b). The resolution widths are approximately 0.006 reciprocal-lattice units (rlu) along $[1\ 0]$ and 0.0002 rlu along $[0\ 1]$.

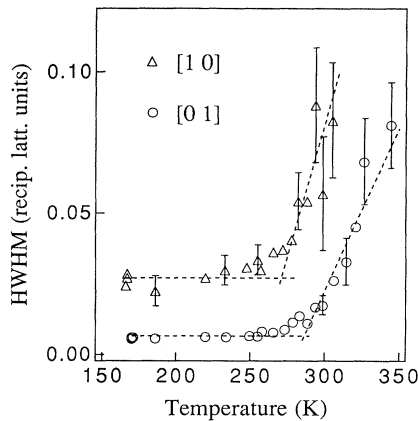


FIG. 3. The temperature dependence of the measured HWHM's (half-widths at half maximum) obtained from the Lorentzian fits to the data (as in Fig. 2) for scans through the (1.75 0.5) peak along the [0 1] direction and [1 0] direction. The dashed lines are guides for the eye and indicate the different saturation temperatures. Error bars are shown on some data points. At low temperatures the errors correspond roughly to the widths of the symbols.

as a function of temperature T . As the temperature is lowered both widths decrease with a similar temperature dependence until they level out at $T \sim 210$ K along [1 0] and at $T \sim 250$ K along [0 1]. The narrowest widths observed were significantly larger than the instrumental resolution, which is 0.006 rlu along [1 0] and 0.0002 rlu along [0 1]. The difference in the two widths indicates that the $c(4 \times 2)$ domains are much larger along the dimer rows than in the perpendicular direction. The fact that the domain sizes have saturated implies that the an-

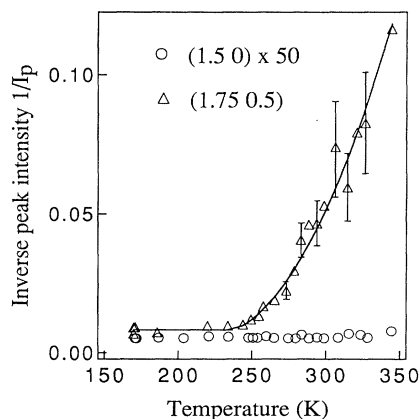


FIG. 4. Temperature dependence of the inverse peak intensity $1/I_p$ of the (1.75 0.5) reflection. The solid line is a guide for the eye. The sharp decrease indicates that a phase transition is occurring. Also shown is $1/I_p$ for the (1.5 0) Bragg reflection, which is actually integrated in the [1 0] direction by the detector resolution (see text) and exhibits a gradual decrease as the temperature is lowered (on an expanded scale). For the low-temperature (1.75 0.5) data and all of the (1.5 0) data the errors are equal to, or less than, the data point size.

tiphase domain boundaries are being pinned, probably by defects or impurities. This is not surprising given that the $c(4 \times 2)$ phase could be suppressed merely by switching on the sample-heater current at low temperatures. Figure 4 shows $1/I_p$ as a function of temperature, where I_p is the measured peak intensity of the (1.75 0.5) reflection. This also steadily decreases as the sample is cooled until it saturates at $T \sim 250$ K. Also shown in Fig. 4 is the $1/I_p$ dependence of the (1.5 0) reflection. On an expanded scale this shows a smooth decrease as the temperature is decreased, in accordance with the temperature dependence of the Debye-Waller factor.²² Due to the sharpness of the (1.5 0) reflection the peak intensity is actually integrated over the [0 1] direction by the detector resolution. However, as the width of the peak is constant with temperature the peak intensity behavior is unchanged. The resolution effects complicate comparison of the $c(4 \times 2)$ and (2×1) intensities where they must be taken fully into account (see Sec. V).

IV. COMPARISON WITH THE 2D ISING MODEL

In order to compare our results with the 2D Ising model, we note that the $c(4 \times 2) \rightarrow (2 \times 1)$ phase transition is equivalent to that of an order-disorder transition in an AB alloy,²³ which can be described by a spin variable which represents the occupation or orientation at a particular site. The structure factors of the two dimer orientations simply replace the coherent scattering lengths in the alloy. Within the phenomenological Landau theory²⁴ the scattering at a $c(4 \times 2)$ lattice position is then approximated by

$$I(q) \propto |F_0(Q) - F_1(Q)|^2 \times \frac{1}{A(T - T_c) + f_{\alpha\alpha}q_x^2 + f_{\beta\beta}q_y^2 + f_{\alpha\beta}q_xq_y}, \quad T > T_c, \quad (2)$$

where q is the reduced wave vector at a specific reflection (e.g., q_x is along [1 0] and q_y is along [0 1]), Q is the total momentum transfer, F_1 and F_0 are the Q -dependent structure factors for the two dimer orientations, $A(T - T_c)$ is an analytic function which is linear near the transition temperature T_c , and the constants f_{ij} represent the coupling constants along and perpendicular to the dimer rows. For scans across the peak, as in Fig. 2, Eq. (2) gives a Lorentzian line shape in q_x and q_y . The width is given by $[A(T - T_c)/(f_{ii})]^{1/2}$ and thus the widths in the different scan directions have the same functional temperature dependence. Their relative magnitude is determined by the coupling constants, which depend on the dimer-dimer interaction energies along and perpendicular to the dimer rows. The experimentally measured widths, shown in Fig. 3, are consistent with this: their temperature dependence is similar at the beginning of the transition, although from the data it is difficult to extract an exact functional form. The discrepancy in scale indicates that the interaction along the dimer rows is considerably stronger than it is between the rows. This anisotropy in the interaction energies may cause the transition to appear as a two-stage transition in the LEED measure-

ments. At lower temperatures saturation of the domain sizes occurs. The temperature dependence of the widths measured by x-ray scattering is essentially the same for q_x and q_y . The only difference is the anisotropic saturation of the domain sizes, probably caused by combination of the defect distribution and the large difference in the interaction energies.⁶ Saturation occurs at a higher temperature (by ~ 20 K) along the $[01]$ direction, i.e., along the dimer rows.

Before attempting to compare our results with those of the 2D Ising model we shall summarize the necessary conditions that a transition must satisfy in order to be expected to display universal critical behavior. Critical behavior only occurs when the correlation length of the fluctuations is considerably larger than the lattice spacing.²³ The temperature dependence of the order parameter can be obtained from the Bragg component of the scattered intensity below the transition temperature T_c . The critical exponents governing the behavior of the correlation length and the static susceptibility are determined from the diffuse scattering above and below the transition. For a two-dimensional system determination of the critical exponents requires measurements of the scattering over at least two orders of magnitude in the reduced temperature within the range $|T - T_c| < 0.3$.²³ It is clear from our data that we are unable to satisfy these conditions. The maximum size attained by the $c(4 \times 2)$ domains is considerably smaller than that of the (2×1) domains which represent the Bragg components in this system (the system is inherently finite due to the change in domain structure that occurs at step edges). The saturation width in Fig. 3 corresponds to a domain size of ~ 50 Å and a correlation length of less than four unit cells. It is therefore inappropriate to try to extract critical exponents from the data.

The exact Onsager solution to the $d=2$ Ising model^{24,25} gives a peak intensity that is inversely proportional to the reduced temperature with a critical exponent $\gamma=1.75$. The $1/I_p$ dependence in Fig. 4 shows a steep gradient as the surface begins to order into the $c(4 \times 2)$ phase before leveling out as the domain sizes saturate. Although it is not possible to determine the critical exponent, the data in Fig. 4 do suggest that a 2D phase transition is taking place. The steep slope at the beginning of the transition indicates that, if saturation did not occur, the curve would cross the temperature axis at a finite temperature T_c characteristic of a 2D phase transition. This effectively excludes the possibility of extracting the stronger dimer-dimer interaction energy by modeling the structure along the dimer rows, where the correlation length is larger, as a 1D Ising system.

V. STRUCTURAL INFORMATION

The structure factors given by the integrated intensities of superlattice reflections, specific to both the $c(4 \times 2)$ and (2×1) phases, contain information about the local structure of the dimers on the germanium surface. The scattering theory that has been developed to describe phase transitions in AB alloys^{23,24} can be adapted to describe the scattering from the Ge(001) surface. If we con-

sider an infinite (2×1) domain and assume that the two dimer orientations (i.e., up and down) are equally likely, then the scattering can be written as

$$I(Q) \propto |F_0(Q) + F_1(Q)|^2 \mathcal{F}_1 + |F_0(Q) - F_1(Q)|^2 \mathcal{F}_2, \quad (3)$$

where \mathcal{F}_1 is a Fourier transform of a lattice of δ functions representing the periodic (2×1) surface and \mathcal{F}_2 is a Fourier transform of the product of the same lattice of δ functions and the pair-correlation function for the two dimer states.^{24,26} $F_0(Q)$ and $F_1(Q)$ are the unit-cell structure factors of the two dimer orientations and are given by²⁰

$$F_i(Q) = f_{\text{Ge}} \sum_j e^{iQ \cdot r_j}, \quad (4)$$

where f_{Ge} is the germanium atomic form factor²⁷ including the Debye-Waller factor and the sum is over the atoms j at positions r_j in the (2×1) unit cell. Equation (3) gives rise to δ functions (\mathcal{F}_1) at the (2×1) reciprocal-lattice points and diffuse profiles (\mathcal{F}_2) which, for the "antiferromagnetic" case [i.e., $c(4 \times 2)$ phase consisting of antiphase domains], lie at the center of the reciprocal-lattice cells [see Fig. 1(b)]. As the (2×1) domains are much larger than the $c(4 \times 2)$ domains, proper inclusion of the (2×1) domain structure does not affect the interpretation of the $c(4 \times 2)$ diffuse scattering but simply gives a finite width to the (2×1) superlattice reflections that is inversely proportional to the domain size [Eq. (1)]. The relative intensities of the different superlattice reflections are determined by the structure factor terms in Eq. (3).

The temperature dependence of the $(1.75\ 0.5)$ reflection has been described above. We also measured other reflections specific to the $c(4 \times 2)$ phase at 170 K, and the results are listed in Table I. Although the widths of these reflections were consistent with the $(1.75\ 0.5)$ peak they were considerably weaker in intensity. For calculation of the in-plane structure factors the Miller index l is set to zero and the unit cell is projected onto the surface plane.²⁸ In this two-dimensional model an asymmetric dimer is then represented by a shift in the center position of the dimer, relative to the second-layer atoms, along the dimer axis. The shift direction depends on the dimer orientation, i.e., the shift is in opposite directions for an

TABLE I. Measured intensities at $c(4 \times 2)$ and $c(2 \times 4)$ reciprocal-lattice points at $T=170$ K. The results are not corrected for instrumental effects but these will only change the relative intensity by 20%, at most, for the reflections shown. The h positions of the reflections are indicated in Fig. 5.

	Surface reflection		$I_{\text{integ}}(I_p \sigma_x \sigma_y)$
	h	k	(arb. units)
(a)	1.75	0.5	1.84
(b)	1.5	0.25	0.15
(c)	1.5	0.75	No measurable peak
(d)	1.5	1.25	No measurable peak
(e)	0.75	0.5	No measurable peak
(f)	1.25	0.5	Weak peak (< 0.02)
(g)	0.25	1.5	0.21

up dimer and a down dimer. In this model a symmetric dimer gives no intensity at the $c(4 \times 2)$ lattice points. Figure 5 shows the h dependence of $|F_0(Q) - F_1(Q)|^2$ for dimers displaced by 0.16 \AA from their center positions. This asymmetry has little effect on the intensity at the (2×1) Bragg reflections. If only the first-layer dimer atoms form the (2×1) unit cell and there is no in-plane rotation of the dimer axis, the structure factor is constant in the k direction. Although the intensity distribution is complicated by introducing shifts in the second layer of atoms, the dominant effect is due to the dimer atoms. A full structural refinement would require measurement of many $c(4 \times 2)$ reflections and second-layer displacements would have to be taken into account.²⁸ For the simple one-layer model the magnitude of the dimer center shift determines the relative amplitudes of the peaks in Fig. 5. The phase is dependent on the dimer bond length and this has already been well established in other studies²⁸ ($d = 2.3 - 2.4 \text{ \AA}$). The measured structure factors in Table I can be projected onto $k = 0.5$ for comparison with Fig. 5 (the arrows indicate the h values of measured reflections). For the $c(4 \times 2)$ peaks the calculated intensity distribution is in qualitative agreement with the measured structure factors listed in Table I. We also note that our results are consistent with the He diffraction measurements of Lambert *et al.*¹¹ They observed rainbow patterns with a similar intensity distribution to that in Fig. 5 and concluded that the $c(4 \times 2)$ phase consisted of slightly tilted dimers.

There has recently been considerable controversy over the nature of the dimers on the Si and Ge(001) surfaces and, in particular, whether or not they are symmetric.³⁻⁵ The situation has been further complicated by the observation of a mixture of symmetric and asymmetric dimers on the Si(001) surface at room temperature using STM.^{2,7}

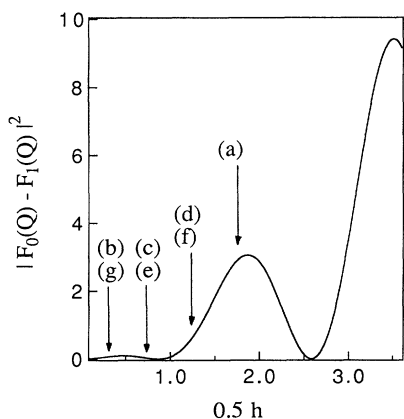


FIG. 5. The h dependence of $|F_0(Q) - F_1(Q)|^2$, the structure factor governing the intensity at $c(4 \times 2)$ reciprocal-lattice points, for an asymmetric dimer model with the dimer center displaced by 0.16 \AA along the dimer axis. The intensity distribution is in good qualitative agreement with the measured structure factors in Table I and with the He diffraction measurements of Lambert *et al.* (Ref. 11). Values of h at which intensities were measured are indicated by arrows and labeled for comparison with Table I.

In our scattering model the integrated intensity at the $c(4 \times 2)$ lattice positions is proportional to the number of buckled dimers. We take the integrated intensity to be given by

$$I_{\text{integ}} = I_{\text{peak}} \sigma_x \sigma_y, \quad (5)$$

where σ_x and σ_y are the widths in the $[10]$ and $[01]$ direction, respectively. This approximation ignores the cross-correlated term in Eq. (2), i.e., $f_{\alpha\beta} q_x q_y$. The integrated intensity of the $(1.75 \ 0.5)$ peak is plotted in Fig. 6 as a function of temperature. Also plotted is the integrated intensity dependence of the $(1.5 \ 0)$ Bragg reflection. Both data sets exhibit a similar temperature dependence, i.e., a gradual decrease as the temperature is raised consistent with increasing surface vibration, which is represented by the Debye-Waller factor. The slightly different gradients may be due to different exponents in the Debye-Waller factors for the dimer and second-layer atoms. There is, however, no sharp decrease in intensity (comparable with the changes observed in Fig. 4) as the surface undergoes the phase transition. The result indicates that the number of buckled dimers involved in the $c(4 \times 2)$ ordering is conserved through the phase transition. This is in agreement with recent photoemission experiments.^{4,29}

In order to build up a picture of the low-temperature surface it is instructive to calculate the intensities at the $(1.5 \ 0)$ and $(1.75 \ 0.5)$ reciprocal-lattice positions and relate these to the measured relative intensities. As the detector integrates over one in-plane direction, the integrated intensity of the $(1.5 \ 0)$ reflection is simply the integral of the

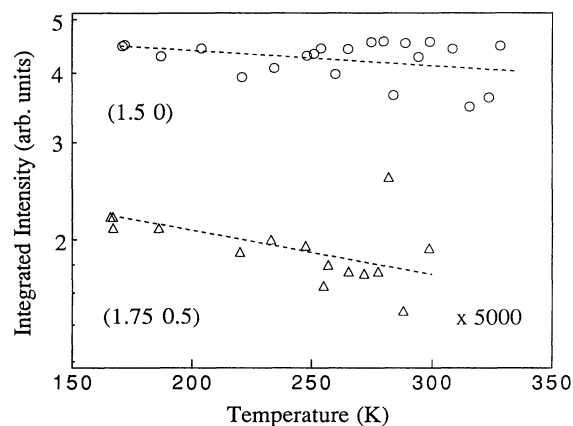


FIG. 6. The approximate integrated intensity of the scattering at the $(1.75 \ 0.5)$ lattice position as a function of temperature and as the surface undergoes the $c(4 \times 2) \rightarrow (2 \times 1)$ transition. In the scattering model the integrated intensity is proportional to the number of buckled dimers on the surface. Also shown is the integrated intensity of the $(1.5 \ 0)$ Bragg reflection. The dashed lines show the approximate slopes of the data sets. As the temperature increases the $(1.75 \ 0.5)$ integrated intensity shows no sharp drop associated with a phase transition in which the dimer structure is changed. This implies that the number of buckled dimers involved in the $c(4 \times 2)$ reconstruction is conserved through the $c(4 \times 2) \rightarrow (2 \times 1)$ phase transition.

Lorentzian line shape, measured in a rocking scan. The integrated intensity of the (1.75 0.5) reflection is harder to evaluate due to the small $c(4\times 2)$ domains. As an approximation, we take the in-plane resolution to be a product of two one-dimensional profiles, a narrow Lorentzian function in the [0 1] direction and a broad Gaussian function in the [1 0] direction. The width of the Lorentzian is estimated to be 0.0002 rlu, from a transverse rocking scan through the (2 0) bulk Bragg reflection. The Gaussian width is 0.006 rlu, measured in a radial scan through the (1.5 0) reflection, and in agreement with calculations using the vertical slit size at the detector.³⁰ Assuming that the scattering function at (1.75 0.5) is the product of two Lorentzians, with widths determined by the domain sizes along [1 0] and [0 1], the resolution can be convoluted with the scattering function in order to simulate the observed scattering. After correction for these resolution effects, comparisons of $|F_0(Q)+F_1(Q)|^2$ and $|F_0(Q)-F_1(Q)|^2$ are in good agreement with the measured intensities at (1.5 0) and (1.75 0.5) (the full numerical details are not reproduced here). Although there are approximations in this calculation the (1.5 0) peak is several orders of magnitude higher in intensity than the (1.75 0.5) peak. The good agreement found indicates that the scattering model [Eq. (4)] provides a reasonable description of the Ge(001) surface.

At low temperatures the surface is incompletely ordered with an antiphase domain structure consisting of $c(4\times 2)$ domains, with the domain boundaries probably pinned by defects. Impurity atoms and step edges may pin dimers into a particular orientation thus changing the effective dimer-dimer interaction energies. This could be the origin of the pinned antiphase domain boundaries. Defects may induce local $p(2\times 2)$ ordering as was observed by STM (Ref. 9) and LEED.¹⁰ Indeed, the boundaries between adjacent $c(4\times 2)$ regions are exactly $p(2\times 2)$ if the boundaries are parallel to dimer rows. The $p(2\times 2)$ reconstruction is predicted to be almost degenerate in energy with the $c(4\times 2)$ phase on the Ge(001) surface.⁶ Scattering due to $p(2\times 2)$ structure would appear at (1.5 0.5) and (2 0.5) in the vicinity of the (1.75 0.5) peak. Although we see no sharp peaks at these positions it is conceivable that very broad scattering could be present, corresponding to very small $p(2\times 2)$ domains (~ 10 Å). It is not possible to determine the relative coverages of $c(4\times 2)$ and $p(2\times 2)$ exactly without a structural refinement of the buckled dimer cell. However, the adequacy of the scattering model described above suggests that the coverage of $p(2\times 2)$ is low. The defects on the surface effectively prevent the complete $(2\times 1)\rightarrow c(4\times 2)$ phase transition. As the temperature is raised the domains become smaller and extra antiphase domain boundaries are introduced with a temperature-dependent

distribution. At room temperature the antiphase $c(4\times 2)$ domains are still quite large along the dimer rows, ~ 80 Å at 290 K, but the row-to-row correlation is small. Above room temperature the surface consists of a disordered array of buckled dimers.

VI. CONCLUSIONS

Using x-ray diffraction, we have investigated the order-disorder transition on the Ge(001) surface by measuring the temperature dependence of the (1.75 0.5) reflection, specific to the $c(4\times 2)$ low-temperature phase. The results indicate that the $(2\times 1)\rightarrow c(4\times 2)$ phase transition corresponds to a 2D phase transition with anisotropic interaction energies along and perpendicular to the dimer rows. However, due to the pinning of the $c(4\times 2)$ domains either by effects or impurity atoms, we are unable to observe any universal critical behavior. The $c(4\times 2)$ domain size saturates before the transition temperature is reached. STM measurements^{8,9} indicate that the Si(001) surface typically has more defects than the Ge(001) surface. This implies that measurement of the critical behavior associated with the $(2\times 1)\rightarrow c(4\times 2)$ phase transition on the Si surface would be extremely difficult.

By analogy with an AB alloy we have developed a scattering model that is qualitatively capable of reproducing the intensity distribution of the measured $c(4\times 2)$ superlattice reflections. The model is consistent with the presence of asymmetric dimers on the surface. At low temperatures the dimers order into $c(4\times 2)$ domains separated by antiphase domain boundaries which correspond to local $p(2\times 2)$ ordering. As the temperature is increased the domain sizes decrease but the number of buckled dimers is conserved. This implies that the (2×1) phase at higher temperatures consists of a random array of buckled dimers.

ACKNOWLEDGMENTS

We would like to thank Roger Cowley and Alistair Bruce for helpful discussions, Kohei Itoh for providing the Ge substrates, and Peter Eng and Ian Robinson for assistance with beamline X16A. We would also like to thank the staff at the NSLS for their hospitality. Beamline X16A is supported by AT&T Bell Laboratories. C.S.D. and D.F.M. acknowledge grants from the Science and Engineering Research Council (UK). Research carried out at the National Synchrotron Light Source, Brookhaven National Laboratory and at the Lawrence Berkeley Laboratory, is supported by the U.S. Department of Energy (DOE Contract Nos. AC02-76CH00016 and AC03-76SF00981).

¹R. E. Schlier and H. E. Farnsworth, J. Chem. Phys. **30**, 917 (1959).

²R. A. Wolkow, Phys. Rev. Lett. **68**, 2636 (1992).

³D.-S. Lin, T. Miller, and T.-C. Chiang, Phys. Rev. Lett. **67**, 2187 (1991).

⁴E. Landemark, C. J. Karlsson, Y.-C. Chao, and R. I. G.

Uhrberg, Phys. Rev. Lett. **69**, 1588 (1992).

⁵R. Cao, X. Yang, J. Terry, and P. Pianetta, Phys. Rev. B **45**, 13 749 (1992).

⁶M. Needels, M. C. Payne, and J. D. Joannopoulos, Phys. Rev. B **38**, 5543 (1988).

⁷R. J. Culbertson, Y. Kuk, and L. C. Feldman, Surf. Sci. **167**,

- 127 (1986).
- ⁸R. J. Hamers, R. M. Tromp, and J. E. Demuth, *Phys. Rev. B* **34**, 5343 (1986).
- ⁹J. A. Kubby, J. E. Griffith, R. S. Becker, and J. S. Vickers, *Phys. Rev. B* **36**, 6079 (1987).
- ¹⁰S. D. Kevan, *Phys. Rev. B* **32**, 2344 (1985).
- ¹¹W. R. Lambert, P. L. Trevor, M. J. Cardillo, A. Sakai, and D. R. Hamann, *Phys. Rev. B* **35**, 8055 (1987).
- ¹²J. Ihm, D. H. Lee, J. D. Joannopoulos, and J. J. Xiong, *Phys. Rev. Lett.* **51**, 1872 (1983).
- ¹³T. Tabata, T. Aruga, and Y. Murata, *Surf. Sci.* **179**, L63 (1987).
- ¹⁴S. D. Kevan and N. G. Stoffel, *Phys. Rev. Lett.* **53**, 702 (1984).
- ¹⁵V. E. Zubkus and E. E. Tornau, *Surf. Sci.* **216**, 23 (1989).
- ¹⁶H. J. W. Zandvliet, D. Terpstra, and A. van Silfhout, *J. Phys. Condens. Matter* **3**, 409 (1991).
- ¹⁷H. J. W. Zandvliet, W. J. Caspers, and A. van Silfhout, *Solid State Commun.* **78**, 455 (1991).
- ¹⁸P. H. Fuoss and I. K. Robinson, *Nucl. Instrum. Methods* **222**, 171 (1984).
- ¹⁹I. K. Robinson, in *Handbook on Synchrotron Radiation*, edited by D. E. Moncton and G. S. Brown (Elsevier, New York, 1991), Vol. 3.
- ²⁰R. Feidenhans'l, *Surf. Sci. Rep.* **10**, 105 (1989).
- ²¹E. Vlieg, J. F. van der Veen, S. J. Gurman, C. Norris, and J. E. Macdonald, *Surf. Sci.* **210**, 301 (1989).
- ²²B. E. Warren, *X-Ray Diffraction* (Addison-Wesley, Reading, MA, 1969).
- ²³R. A. Cowley, *Methods of Experimental Physics* (Academic, London, 1987), Vol. 23, Part C, Chap. 18.
- ²⁴A. D. Bruce and R. A. Cowley, *Structural Phase Transitions* (Taylor & Francis, London, 1981).
- ²⁵M. E. Fisher, *Rep. Prog. Phys.* **30**, 615 (1967).
- ²⁶For a formal derivation of the scattering from a two-state system, see C. S. Lent and P. I. Cohen, *Surf. Sci.* **139**, 121 (1984).
- ²⁷The atomic form factor for germanium is obtained from a polynomial fit to the values given in *The International Tables for X-Ray Crystallography* (Kynoch, Birmingham, UK, 1968), Vol. 3.
- ²⁸F. Grey, R. L. Johnson, J. Skov-Pedersen, R. Feidenhans'l, and M. Nielsen, in *The Structure of Surfaces II*, edited by J. F. van der Veen and M. A. van Hove (Springer-Verlag, Berlin, 1988).
- ²⁹G. LeLay, J. Kanski, P. O. Nilsson, U O. Karlsson, and K. Hricovini, *Phys. Rev. B* **45**, 6692 (1992).
- ³⁰For a detailed discussion of the resolution function, see G. Renaud, P. H. Fuoss, J. Bevk, and B. S. Freer, *Phys. Rev. B* **45**, 9192 (1992).